

1 Assessing the mean output rate (MOR) of past
2 effusive basaltic eruptions – a look at the
3 postglacial volcanism of the Reykjanes Peninsula
4 in Iceland

5 Birgir V. Óskarsson^{1*}, Robert A. Askew¹ and
6 Halldór Guðmundsson¹

7 ^{1*}Icelandic Institute of Natural History, Urriðaholsstræti 6–8, Garðabær,
8 110, Iceland.

9 *Corresponding author(s). E-mail(s): birgir@ni.is;

10 **Abstract**

11 Volcanological approaches for assessing the effusion rate of past effusive volcanism
12 are of great importance, to enable proper evaluation of the eruption magnitude
13 and past tectono-magmatic conditions which are relevant for mitigating future
14 volcanism. The reactivation of volcanism on the Reykjanes peninsula in 2021 after
15 an 800-year hiatus, has incited the need for assessing the potential scale and size of
16 future effusive eruptions on the peninsula. With a compilation of the planimetric
17 area of 154 postglacial monogenetic lava fields, and volcanological constraints on
18 these fields, the heat flow model of [Pieri and Baloga \(1986\)](#), as utilized in [Harris
19 and Rowland \(2009\)](#) was used to assess the mean output rate (MOR) of these
20 eruptions, providing insights into the overall effusive capacity of the peninsula.
21 Methods for a qualitative evaluation of the eruption duration of past eruptions are
22 introduced, along with a power regression derived from a the surface temperatures
23 and time extracted from recent eruptions in Iceland, allowing for a theoretical
24 approach to the thermal stage of lava fields with unknown emplacement history.
25 Our first-order assessment on the Reykjanes peninsula indicates that 10% of the
26 eruptions have MOR < 1 m³/s, 35% in between 1 and 10 m³/s, 44% between 10
27 and 50 m³/s, 8% between 50 and 100 m³/s and 3% between 100 and 200 m³/s.

28 The eruption frequency has undergone minor variations in postglacial time, the
29 only significant variation being the occurrences of long-lived (<5 years) shield
30 eruptions in early and mid Holocene, but short-lived (days to months) fissure-
31 fed volcanism dominated in the late Holocene, with MOR $10\text{--}50\text{ m}^3/\text{s}$. The
32 results show the potential scales of future effusive activity on Reykjanes if current
33 tectono-magmatic conditions remain the same.

34 **Keywords:** Mean output rate, Past effusive volcanism, Reykjanes peninsula

35 1 Introduction

36 Effusion rate (discharge rate) is defined as the amount of lava erupted at a given time
37 in effusive eruptions (e.g. [Harris et al, 2007](#)). The rate is controlled by subsurface
38 conditions such as density buoyancy ([Mériaux and Jaupart, 1998](#); [Hartley and MacLen-](#)
39 [nan, 2018](#)), local stresses ([Gudmundsson, 2006](#)), overpressure in magma chambers or
40 reservoirs ([Geshi et al, 2020](#)), the anatomy of the plumbing system and dynamics of
41 magma ascent ([Geshi, 2005](#)), and give an indication of the tectono-magmatic pro-
42 cesses controlling volcanism at each place (e.g. [Tibaldi, 2015](#)). Today, effusion rates
43 is a key parameter for modeling lava flow emplacement (e.g. [Harris and Rowland,](#)
44 [2001](#); [Vicari et al, 2009](#); [Bilotta et al, 2012](#); [Cappello et al, 2016](#); [Chevrel et al, 2018](#);
45 [Pedersen et al, 2023](#)), therefore assessing the effusion rate is important for under-
46 standing volcanic systems in general, with great implications for hazard assessment.
47 During an effusive eruption, the instantaneous effusion rate is measured on-site, in
48 open channels or skylights (e.g. [Pinkerton and Sparks, 1976](#); [Calvari et al, 2002](#)), or
49 the time-averaged discharge rate (TADR) estimated from temporal volumetric mea-
50 surements using satellite data ([Harris et al, 2000, 2011](#)) or vertical aerial imagery
51 ([Pedersen et al, 2022](#)). After the eruption, or for past eruptions with documented
52 duration, a mean output rate (MOR) can be estimated derived from the total volume
53 of the lava field divided by the total eruption duration ([Harris and Rowland, 2009](#)), or
54 eruptions without a record of duration or even volume, estimates of the MOR can be

55 assessed from the relationship between the planimetric area of the lava field and effu-
56 sion rate. One equation that shows this relationship is the equation of [Pieri and Baloga](#)
57 [\(1986\)](#), built on studies on length of lava flows versus effusion rate (e.g [Walker, 1973](#))
58 further developed in ([Harris and Rowland, 2009](#)) that includes the radiative history
59 of the eruption reflected in instantaneous or average surface temperatures, imperative
60 to controlling the cooling-limit of the flow.

61 Renewed volcanism on the Reykjanes peninsula, with the eruption of Fagradalsfjall
62 in 2021, after an 800 year hiatus, has raised concerns about the imminent risk of
63 the reactivation of all volcanic systems. Previous volcanic episodes in the Reykjanes
64 peninsula, cycling at intervals of 800–1000 years, activated volcanism in all volcanic
65 systems ([Sæmundsson and Sigurgeirsson, 2013](#)). Thus, a new episode may lead to
66 widespread volcanism on the peninsula, imposing hazards on the population of the
67 area, including popular tourist destinations, the international airport and significant
68 risk to other essential infrastructure. To evaluate the potential magnitude of future
69 eruptions in the peninsula that can be used for risk management and simulating lava
70 emplacement, a realistic estimate of the MOR of past Reykjanes eruptions is needed.

71 This study explores the usage of a thermal model presented in [Harris and Rowland](#)
72 [\(2009\)](#) for assessing the eruption capacity from the MOR, that hinges primarily on two
73 unknown parameters, planimetric area and surface temperature of the flow. The area
74 of the lava flows can be measured directly or estimated, however, the thermal history
75 expressed in the surface temperature of the flows has not been investigated for past and
76 prehistoric eruptions on these terms. This study explores ways for assessing the ther-
77 mal history from the degree of maturation of lava fields using field-based volcanological
78 and morphological observations. These observations are then compared to a theoret-
79 ical relationship between surface temperatures and time extracted from documented
80 eruptions in Iceland. Knowing the time it takes for a lava to achieve certain maturity
81 and surface temperatures, allows for a qualitative correlation between emplacement

82 time and the time that it takes to form morphological features within the flow fields.
83 This relationship opens for further constraints on the nature and time of emplace-
84 ment of unknown eruptions, and assessment of MOR giving a more comprehensive
85 evaluation of the eruption history of volcanic regions in general.

86 2 Geological Setting

87 The Reykjanes peninsula in Iceland is part of the Western volcanic zone (WVZ)
88 the onshore continuation of the mid-Atlantic ridge that transects the country south-
89 west to north (Gudmundsson, 1986; Sigmundsson, 2006). The spreading center on the
90 Reykjanes peninsula overprints a transform zone, which results in divergent spreading
91 combined with north-south right-lateral slip faulting (Keiding et al, 2009; Sæmunds-
92 son et al, 2020) with *en echelon* volcanic systems bearing SW–NE 25–35° oblique to
93 the spreading center. The volcanic systems that are 30–50 km long and 5–8 km wide
94 have been divided into six after the presence of fissure-swarms, grabens, seismic activ-
95 ity, volcanic edifices, craters and geothermal activity, and are: Reykjanes, Svartsengi,
96 Fagradalsfjall, Krýsuvík-Trölladyngja, Brennisteinsfjöll, and Hengill (Sæmundsson
97 and Sigurgeirsson, 2013). However, the boundary between adjacent systems is not clear
98 and different arrangements have been presented (Jakobsson et al, 1978), for exam-
99 ple, Reykjanes and Svatsengi have sometimes been classified as the same system (),
100 and Fagradalsfjall was only recently recognized as a system (Gee, 1998; Sæmundsson
101 and Sigurgeirsson, 2013). The Reykjanes peninsula is the most active segment of the
102 WVZ with over 200 eruptions in postglacial times, while the northern segment around
103 Langjökull only facets about 26 eruptions but with lava flows of larger areal cover-
104 age and volume (Jakobsson, 2013). The exposed basement rock of the peninsula is of
105 Plio-Pleistocene age with alternating hyaloclastite deposits and lava flows, the latest
106 Pleistocene subglacial eruptions form prominent ridges and tuyas on the peninsula.

107 Effusive eruptions in the last 3500 years BP have been cyclical, with intervals of 800–
 108 1000 years, each period lasting 200–400 years, the latest eruption period occurring
 109 from 800–1200 BP (Sæmundsson and Sigurgeirsson, 2013; Sæmundsson et al, 2020).
 110 Postglacial volcanism is basaltic, lava shields being either picrite or olivine tholeiite in
 111 composition and fissure volcanism being tholeiitic (Jakobsson et al, 1978). The picrites
 112 and some of the shields on the peninsula form the oldest formations of postglacial
 113 volcanism and have been interpreted as the result of enhanced partial melting of the
 114 Icelandic mantle with isostatic crustal adaptations following the Weishelian deglaciation
 115 (Jull and McKenzie, 1996; Andrew and Gudmundsson, 2007; MacLennan et al,
 116 2002; Rees Jones and Rudge, 2020).

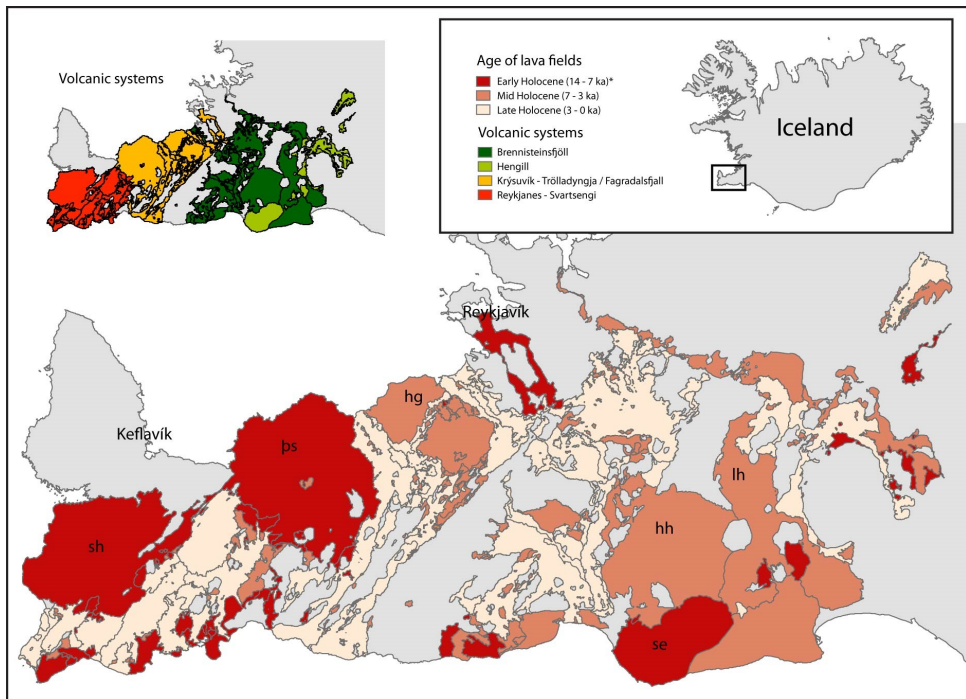


Fig. 1 Map of the Reykjanes peninsula. The map shows the lava fields of this study classified after age and volcanic systems. Ages are inferred from carbon dating, tephrochronology and stratigraphy. Late Pleistocene lavas from 14–12 ka are classified with early Holocene, and not differentiated for simplification. Acronyms of largest shield volcanoes shown for reference: sh - Sandfellshæð, ps - Práinskjöldur, hg - Hrútagjá, hh - Heiðin Há, se - Selvogsheiði and lh - Leitahraun.

117 3 Methods

118 This study compiles the planimetric area of 154 monogenetic lava fields from eruptions
119 within the Reykjanes peninsula, published by the Icelandic Institute of Natural His-
120 tory (<https://serstokvernd.ni.is/>) and available in the repository of the National Land
121 Survey of Iceland (<https://gatt.lmi.is/>). The database includes shapefiles with poly-
122 gons of the lava fields, information about the volcanic system to which the lava fields
123 belong, and their estimated age. The ages are historical or determined with C14 dat-
124 ing and tephrochronology (e.g. Jóhannesson and Einarsson, 1988b,a; Einarsson et al,
125 1991; Sinton et al, 2005). Other ages were inferred from the position of the lava flows
126 in the stratigraphy. Additional information about the type of lava, vent types and
127 locations and predominant morphologies were extracted from aerial imagery (Loft-
128 myndir ehf.) and miscellaneous publications (maps, thesis, reports, and articles). The
129 geological map and report of Jónsson (1978) provided most information on each lava
130 field’s vents. The most up-to-date information on age and stratigraphy was found in
131 the 2016 geological map of Reykjanes from Iceland GeoSurvey (Sæmundsson et al,
132 2016). The area of lava fields that were partly buried by other lava fields were esti-
133 mated from the visible extent of the lava fronts or from kipukas. For simplification,
134 the lava fields in this study are subdivided into four areas comprising the six systems,
135 Reykjanes-Svartsengi are placed together, Krýsuvík-Trölladyngja and Fagradalsfjall,
136 Brennisteinsfjöll, and Hengill systems.

137 3.1 Equation

138 To assess the MOR, the equation of Pieri and Baloga (1986) as adapted in Harris and
139 Rowland (2009, eq. 20) was rewritten to:

$$140 \quad E = \frac{A[\sigma\varepsilon(T_{surf}^4 - T_{amb}^4) + h_c(T_{surf} - T_{amb})]}{141 \quad \rho(\Lambda\phi + \Delta T c_p)}. \quad (1)$$

142 The equation is built on a relationship between effusion rate E and/or thermal
 143 insulation T_{surf} , which is expressed in the potential of the area A of a lava field to
 144 grow with increasing insulation before coming to halt. The function also shows that
 145 for a given eruption rate, after the flows reach their maximum cooling-limited length,
 146 with added volumes the flow will begin to pond and widen increasing the flow area
 147 (Lopes and Guest, 1982). For the purposes of assessing the MOR of past effusive
 148 eruptions with little knowledge of their eruption history, the parameters are selected
 149 theoretically and not on a case-to-case basis. The parameters used which would be
 150 representative for Icelandic basaltic eruptions are from Krafla flows (Harris et al, 2007)
 151 and are summarized in Table 1.

Table 1 Lava parameters used in this study

Stefan Boltzmann constant σ	$5.67 \times 10^{-8} \text{ W m}^{-2} \text{ K}^{-4}$
Emissivity ε	0.95
Density ρ	2600 kg m^{-3}
Latent heat of crystallization Λ	$3.5 \times 10^5 \text{ J kg}^{-1}$
Crystallization ϕ	45 %
Heat capacity c_p	$1230 \text{ J kg}^{-1} \text{ K}^{-1}$
Convective heat transfer coefficient h_c	$10 \text{ W m}^{-2} \text{ K}^{-1}$
Ambient temperature T_{amb}	277.15 K (4°C)
ΔT	200 K (200°C)
Surface temperature (T_{surf})	323.15 K (50°C) Shield volcanoes (1330 days, 3.6 years) 363.15 K (90°C) Fissure eruptions and smaller shields (180 days) 471.15 K (198°C) Short-lived eruptions (20 days) 673.15 K (400°C) Short-lived eruptions (2 days) 803.15 K (530°C) Short-lived eruptions (1 day)

152 For example the convective heat transfer coefficient is set to h_c $10 \text{ W m}^{-2} \text{ K}^{-1}$
 153 but can be greater if the lava is affected by wind and rain. Ambient temperature
 154 during the eruption T_{amb} is set to 277.15 K (4°C), the annual mean temperature of
 155 Iceland (Einarsson, 1984), although actual ambient temperatures may have been in
 156 the range from subzero temperatures to warmer summer temperatures. Nevertheless,
 157 slight changes in T_{amb} are not significant in affecting the MOR estimate. A maximum
 158 post eruption crystallization is assumed to be 45% (Harris and Rowland, 2009). Two

159 values that are significant and inferred in our calculations, are the surface temperature
 160 (T_{surf}) which is an expression of the crustal maturity and thermal insulation of the
 161 lava field during the eruption, and the ΔT which is the temperature difference between
 162 eruption temperature and core temperature for the flow to reach its cooling-limit
 163 and come to halt. ΔT is usually set to be around 200 K (200°C) but could vary
 164 slightly between flows after emplacement style (Harris and Rowland, 2009). Because
 165 our eruptions have unknown history and duration, we need to rely on best estimate of
 166 T_{surf} . Eruption rate is based on bulk volumes and thus requires further corrections
 167 for voids and vesicles if used in other contexts, as for calculating volatile emissions.

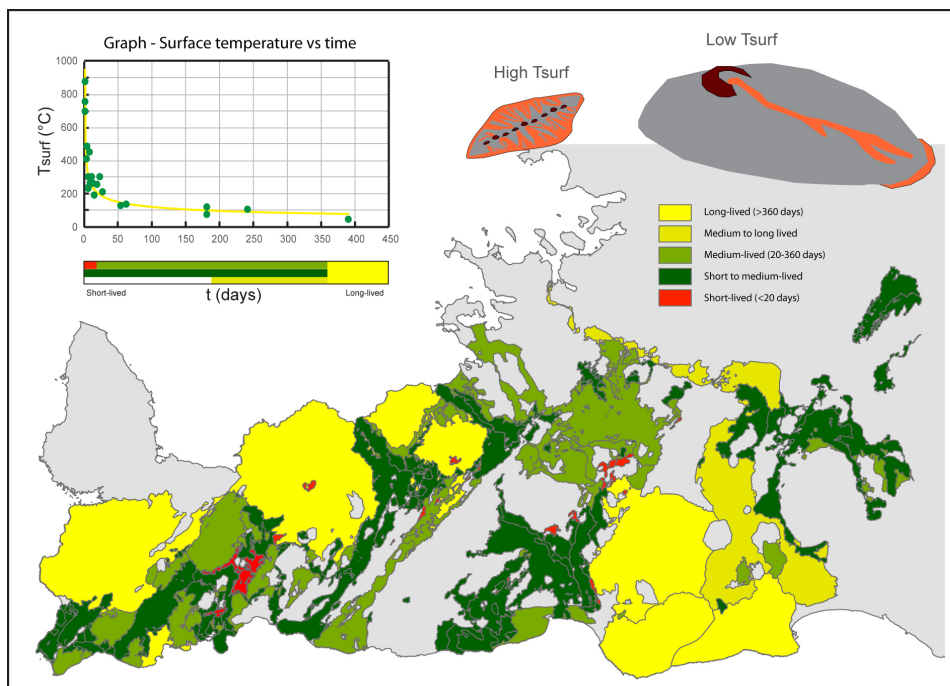


Fig. 2 Map of the Reykjanes peninsula showing based on a qualitative assessment of the longevity of the eruptions from the morphology of the vent systems and lava fields. The assessment is used for selecting the best range for T_{surf} derived from the power equation (top left). Top right corner: Illustration of how the crustal maturation of the lava fields through the course of the eruptions induces insulating emplacement and affects the surface temperature.

168 4 Results

169 The lava fields used in this study are distributed within the following volcanic sys-
170 tems (see Table S1 of the supplementary file): 50 (32.5%) in the Reykjanes-Svartsengi
171 volcanic systems, 45 (29.2%) in the Krýsuvík-Trölladyngja systems, 48 (31.2%) in the
172 Brennisteinsfjöll system and 11 (7.1%) in the Hengill system. The total number of
173 lava fields formed since postglacial times is not known but in the report of Jónsson
174 (1978) additional 50 or so lava fields are counted, of which eight are interpreted as
175 being lava shields, thus the total number is over 200. The morphological analyses of
176 the lava flows shows that 61.3% of the lava fields are pahoehoe, 8.1% a'a, 14.4% mix-
177 tures of pahoehoe and brecciated facies, and 16.3% was undefined. Areal coverage of
178 the lava fields ranges from 0.008–147 km² with average of 10 km². Estimated volumes
179 for 51 lava fields give ranges from 0.0013 km³–6.8 km³ and an average of 0.7 km³
180 (Jónsson, 1978). Of the lava fields, 148 area single lava flows or small shields with vol-
181 umes <0.7 km³ and 6 are large shields > 1 km³. 28 lava fields have documented lava
182 tubes according to the interactive map of the Icelandic Institute of Natural History
183 (www.ni.is) including the 2021 lava field at Fagradalsfjall.

184 4.1 Evaluating the planimetric area of the lava fields - Cooling 185 or volume-limited flows?

186 Of the 154 lava fields, 58 are partly or almost entirely buried underneath other lava
187 flows and their planimetric area had to be estimated. Of these, 42 have over 50% of
188 their estimated fields buried, 7 had between 30–50% buried and 9 under 30%. Most of
189 these buried lava fields have lava fronts or kipukas that are well mapped and correlated
190 with eruption vents or areas (Jónsson, 1978; Sæmundsson et al, 2016), but 18 lava
191 fields with vent areas buried needed to have their source vents inferred, and they were
192 drawn to the nearest fissure system. The areal sizes derived from the estimations are

193 approximations only, but do fall well into the sizes of the lava fields that are entirely
194 exposed.

195 About 40 lava fields extend to the ocean, meaning part of the lava that erupted
196 was lost into the ocean. The bathymetry map of southwest Reykjanes shows that
197 the lava field of Eldvörp extends 3.3 km² into the ocean (or 15% of its total area)
198 and Ögmundarhraun about 8.9 km² (or 30% of its total area) (Ögmundur Erlendsson
199 pers. com. 2021). Judging from the location of the majority of the volcanic vents
200 that are found towards the central areas of the peninsula and the areal distribution
201 of the lava fields, most lava flows seem to have reached their cooling-limit before
202 entering the ocean, indicating that those eruptions that entered the ocean and were
203 volume-limited (ocean-limited), were potentially close to their cooling-limit and the
204 subaqueous area lost is considered small. The vents closest to the ocean are found
205 within the Reykjanes-Svartsengi systems, where 20 lava fields seem to have entered
206 the ocean and their subaqueous area loss is more significant. However, from the small
207 size of these fields, even if the areas of these flow fields were doubled, the MOR would
208 be largely confined to 1–10 m³/s which is likely representative of the volcanism of
209 this region, as discussed below. Another factor affecting the cooling-limit of lava is
210 topography. Reykjanes peninsula has a general shallow increase in slope inland with
211 low-relief planes in between the small 100–300 m high hyaloclastite tuyas and ridges
212 which indicates most of the flows did flow towards the ocean and were not confined
213 by topographic barriers. But as observed in Fagradalsfjall eruption in 2021 where lava
214 filled valleys until spilling over (Pedersen et al, 2022), eruptions of longer duration
215 (weeks to months) should be expected to overcome local topography and extend to
216 reach their cooling-limit.

217 4.2 The relationship between crustal surface temperatures and 218 time - a theoretical approach

219 In this study, we derived by iteration T_{surf} from equation 1 using data from recent
220 eruptions in Iceland with known emplacement history, duration, and MOR and using
221 the physical parameters above for Icelandic lava flows (see Tables 1 and 2). From
222 these results, Newton's law of cooling (Newton, 1929) is seen expressed in the power
223 regression of T_{surf} and time (Fig 1),

224

$$225 \quad T_{surf} = 529.38t^{-0.328} \quad (2)$$

226

227 where t is time in days and T_{surf} is temperature in degrees Celsius. The regression
228 has a strong correlation ($R^2 = 0.91$), and is thought to portray the gradual maturation
229 and increase insulation of the lava fields during the course of the eruptions. Inter-
230 estingly, the type morphology of the lava flows and the compositional variation from
231 basaltic to andesitic has minimum effect on the correlation. This equation shows that
232 the most significant variation in T_{surf} occurs during the first days of the eruption,
233 eruptions lasting a day have T_{surf} of about 500°C , while eruptions reaching about 20
234 days have T_{surf} about 200°C . Passing 20 days to about an year the temperature slope
235 declines gradually within a narrower range of T_{surf} $200\text{--}70^\circ\text{C}$, and to reach crustal
236 temperatures of 30°C the duration is greater than 17 years. These crustal tempera-
237 tures would reflect the maturation and cooling of the core of the flow fields with time
238 (Fig. 2). The regression has been tested against the MOR determined from volumet-
239 ric calculations from photogrammetry surveys in the recent eruptions on Reykjanes
240 (Pedersen et al, 2022, 2024) with good results, and can become a useful tool in lava
241 simulation and forecasting, a topic discussed for another publication.

242 The differing type of emplacement mode and magnitude of output rates in the
243 eruptions of Table 2 explains the minor variation in T_{surf} between flows with same

Table 2 Time-based surface temperatures derived from documented volcanic eruptions in Iceland

Eruption	Area (km ²)	MOR (m ³ /s)	Duration (days)	T _{surf} (°C)
Holuhraun 2014–2015	84.0	90 ¹	180	72
Fagradalsfjall 2021	4.8	9.5 ²	180	117
Merardalur 2022	1.2	7.2 ⁷	18	253
Litli-Hrútur 2023	1.5	6.7 ⁷	26	209
Sundhnúksíggar 2023	3.4	50.0 ⁷	2.5	409
Laki 1783–1784	600	700–1000 ³	240	103
Fimmvörðuháls 2010	1.3	10 ⁴	22	300
Hekla 1947–48	38.9	22 ⁵	389	43
Hekla 1970	17.1	40 ⁵	61	134
Hekla 1980	22.6	479 ⁵	3	484
Hekla 1981	4.4	78 ⁵	7	449
Hekla 1980–81	24.5	197 ⁵	10	300
Hekla 1991	24.7	53 ⁵	53	125
Hekla 2000	14.6	92 ⁵	12	261
Krafla 1975 Dec 20	0.36	18.5 ⁶	0.21 (<6 hr)	695
Krafla 1977 Sept 8	0.8	77.8 ⁶	0.17 (<5 hr)	875
Krafla 1980 Mar 16	1.3	83.3 ⁶	0.25 (<7 hr)	755
Krafla 1980 Jul 10–18	5.3	34 ⁶	8	263
Krafla 1980 Oct 18–23	11.5	59 ⁶	5	230
Krafla 1981 Jan 30–Feb 4	6.3	50.9 ⁶	5	300
Krafla 1981 Nov 18–23	17	91.9 ⁶	5	236
Krafla 1984 Sept 4–18	24	91 ⁶	14	189

¹(Pedersen et al, 2017)

²(Pedersen et al, 2022)

³(Thordarson and Self, 1993)

⁴(Edwards et al, 2012)

⁵(Pedersen et al, 2020)

⁶(Harris et al, 2000)

⁷(Pedersen et al, 2024)

244 eruption duration differing slightly in their thermal history. For example the difference
245 in T_{surf} of Holuhraun and Fagradalsfjall, eruptions that lasted the exact number of
246 days or 180 days, is of about 45°C, Holuhraun being ten-times larger in terms of effu-
247 sion rates and predominantly rubbly and a’*a* (Pedersen et al, 2017; Voigt et al, 2021)
248 and Fagradalsfjall predominantly pahoehoe with mixtures of flows with disrupted and
249 brecciate crusts.

250 Yet the time-dependent relationship is clear from the regression. The Hekla lava
251 fields of basaltic andesite and andesite compositions (Pedersen et al, 2020), flows
252 formed in eruptions of long duration (over 50 days), had T_{surf} around 125°C, while

253 lava flows that formed in eruptions of short duration (1–10 days) have T_{surf} in
254 the range of 200–500°C. In addition, Krafla fissure eruption, which had a maximum
255 longevity of 14 days (Harris et al, 2000), have T_{surf} range from 189°C for the longest
256 eruption to 875°C for the shortest (a few hours). Thus, T_{surf} of 70–200°C seems apply
257 for flows that are medium-lived and developed crustal maturity with insulation, while
258 higher crustal temperature values are expected from short-lived lava flows which are
259 more difficult to ascertain without knowledge of the history of that eruption. On the
260 other end, values of T_{surf} around 30–70 °C would apply to lava fields formed over
261 several years, as expected for the largest shield volcanoes.

262 4.3 The duration of past eruptions analyzed qualitatively

263 For the purposes proposed, T_{surf} needs to be pinpointed for each eruption and the
264 power relationship can aid us in finding a value of T_{surf} that reflects the eruption
265 duration, established qualitatively from the morphology of the lava fields and vents.
266 For example, the occurrence of well-preserved rows of small scoria and spatter cones
267 along well-delineated fissures would indicate the eruption was relatively short-lived
268 with minimal fissure shortening and coalescence of vents. The occurrence of fewer and
269 larger scoria cones would suggest the eruption duration was prolonged enough to allow
270 for closing of the fissures and coalescence of vents, while a large single crater would
271 indicate a moderately to long-lived eruption. The subsequent burial of the vents by lava
272 flows from the central crater would indicate further a prolonged eruption. The aspect
273 ratio (the length of the vent system divided by the length of the lava field) can also
274 indicate eruption duration, where a field with a low aspect ratio (a.r. <1), where the
275 vent system is much shorter than the length of the flow field, would be indicative of a
276 longer eruption, while a vent system equal or larger than the width of the flow field (a.r.
277 >1) would be indicative of a short-lived eruption. The morphology of the lava fields
278 can also give an indication of duration, and it could be argued that because >70% of

279 the lava fields are pahoehoe with numerous anastomosing lobes placed horizontally and
280 sometimes vertically as in the case of the lava shields, and showing crustal maturity
281 with insulated emplacement and inflation structures such as lava-rise plateaus, lava-
282 rise pits and tumuli, that these eruptions were relatively long-lived (Hon et al, 1994).
283 In the Holuhraun eruption, documented bulged inflation structures first appeared after
284 26 days, while the northern and oldest sector of the lava field was heavily inflated in
285 the fourth-month (Pedersen et al, 2017). Brecciated fields would suggest origin by high
286 fountaining, vent instabilities and/or a topographic control inducing higher cooling
287 rates with respective shearing and brecciation (Sparks and Pinkerton, 1978; Soule
288 et al, 2004), eruption phases usually associated with immature systems and short to
289 moderately-lived eruptions. Lava-tubes would also be indicative of greater longevity
290 whereas well-developed internal pathways take time to be established, despite this,
291 hollow sheet lobes may start forming within a few days of emplacement (Hon et al,
292 1994).

293 With the morphological aspects assessed, a map was drawn showing inferred erup-
294 tion duration for each field (Fig. 2), that aids in selecting a T_{surf} that approximates
295 the respective thermal state of the lava fields. The map shows that the majority of
296 the fissure eruptions fall into short to medium longevity (dark green to green). T_{surf}
297 is classified into four categories as seen in Table 2 spanning representative eruption
298 duration. Due to the shallow slope of the regression for the medium range, a value
299 for T_{surf} of 93°C is likely to approximate the true T_{surf} . This value approximates
300 the MOR for Holuhraun 2014–15, Laki 1783–84 and Fagradalsfjall 2021 even though
301 they differ to some extent in composition ranging from primitive olivine tholeiites to
302 more evolved tholeiites, and differ in morphology and emplacement history. This adds
303 confidence that the selected value applies to the medium-lived lava fields. Fields in
304 the category short-lived (red) would fall in the range with larger variability of higher
305 T_{surf} , which is more difficult to assess, and a value of 400°C was used for very short

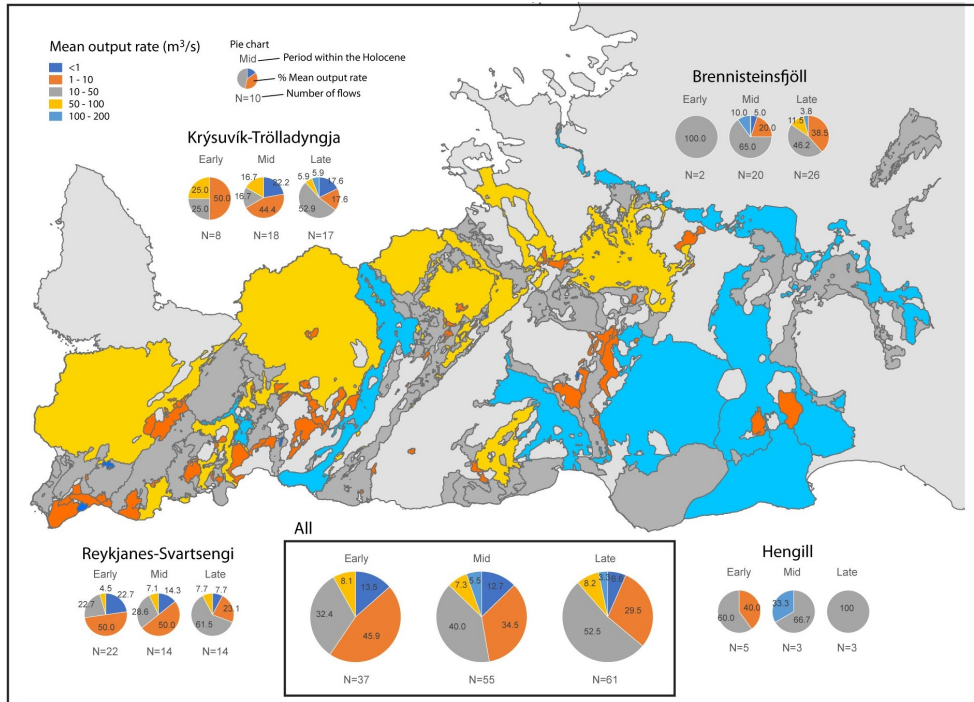


Fig. 3 Map of the Reykjanes peninsula showing the calculated MOR for all lava fields and pie-charts showing the percentage MOR distribution within each system and for all the systems. Inferred age of the lava fields is given in Figure 1 and the volcanic systems they belong.

eruptions between 1 and 2 days and 198°C for eruptions inferred to 20 days. The small red fields may represent single eruption events, although they seem likely remote segments of larger fissure eruptions. The yellow fields are long-lived shield volcanoes, and a value of T_{surf} of 50°C which would represent 3.6 years of eruption was used. This value is potentially more applicable to the shields, but for simplification was used for all shields with volumes larger than 1 km³. Smaller shields under 1 km³, due to their resemblance with the 2021 Fagradalshraun, were included in the medium-lived category.

4.4 Estimated mean output rates

The combined qualitative assessment given in Table S1, and best estimate of T_{surf} (Table 2) yielded the following results: 10% of the eruptions have MOR < 1 m³/s,

317 35% in between 1 and 10 m³/s, 43% between 10 and 50 m³/s, 8% between 50 and 100
318 m³/s and 3% between 100 and 200 m³/s. These values can be further evaluated after
319 age and a summary is given in Figure 3. Table S1 also provides the uncertainty range
320 for each eruption, based on the T_{surf} of two adjacent time slots. The time slots were
321 1 day, 2 days, 20 days, 50 days, 180 days, 365 days, 1330 days (3.6 years) and 6320
322 (17 years). If for example the assigned T_{surf} was 93°C, the temperature at day 180,
323 the uncertainty range used would be from day 50 to day 365 and so forth.

324 The westernmost systems have the largest percentage of eruptions under 10 m³/s
325 while the number of eruptions in between 10–50 m³/s increases to the east and in late
326 Holocene. The distribution of eruptions with MOR above 50 m³/s is even through-
327 out the Holocene, the only difference is the size and volume of the formations, the
328 largest shield-forming eruptions confined to the early and mid-Holocene. Many fields
329 with MOR lower than 1 m³/s may have been segments of larger fissures or belong to
330 events with multiple eruptions, "fires" within the same event, similar to the Fagradals-
331 fjall fires that formed Fagradalshraun in 2021, Meradalir in 2022 and Litli-Hrútur in
332 2023, Krýsuvík fires that formed Kapelluhraun, Ögmundahraun, Mávarhlíðarhraun
333 and Lækjarvellir (Einarsson, 1991) and not represent single eruptions. Lava fields that
334 flowed both north and south as Afstapahraun and Leitahraun, with MOR up to 200
335 m³/s will have lower MOR if each branch was unidirectional and formed at different
336 times. In the same manner, if Kapelluhraun, Mávarhlíðarhraun and Ögmundahraun
337 erupted simultaneously, the the MOR would approximate the MOR of Afstapahraun.
338 Slightly different ages for the north and south of Leitahraun lava fields suggest that
339 the eruption comprises more than one eruption episode (Sæmundsson et al, 2016),
340 which would lower the MOR by about half.

341 5 Discussion

342 5.1 The eruption capacity of the Reykjanes Peninsula

343 Assessing the MOR on a regional scale is a useful way to acquire an overview of the
344 potential or past effusive capacity of a given area, even though some uncertainty is
345 expected. The general picture from this assessment on the Reykjanes peninsula is of
346 moderate background activity on which about 80% of the eruptions is under $50 \text{ m}^3/\text{s}$,
347 yet this eruption activity is punctuated with larger eruption episodes in all volcanic
348 systems that reach $>100 \text{ m}^3/\text{s}$ which would have imposed greater hazards (Fig. 3).
349 Both the largest fissure eruptions and the shield forming eruptions did give similar
350 range of MOR, which indicates that the range represents an upper limit to the expected
351 effusion rate in the region, the only differing factor being the duration of the erup-
352 tions. What controls the longevity is thus an important factor to be explored. Most
353 eruptions have been relatively short to medium-lived fissure eruptions with vents cen-
354 tralized in the Peninsula, whereas shield-forming eruptions were predominantly found
355 in the early and mid-Holocene with vents more scattered within the Peninsula. From
356 the mid-Holocene the frequency of fissure eruptions with higher MOR increases, but
357 none are long-lived enough to develop into shields. The early picritic and shield form-
358 ing phase has been explained with high melt production the result from isostatic uplift
359 following the deglaciation (Gudmundsson, 1986; Maclennan et al, 2002), yet the shield
360 volcanism in the middle Holocene has an unclear causation. Judging from the volume
361 of the hyaloclastite ridges and tuyas on the peninsula which give a window into the
362 pre-deglaciation volcanism and would reflect to some extent the background volcan-
363 ism, the volume and areal distribution of these edifices increases from west to east. A
364 similar picture is acquired from the MOR assessment when the effect of the deglacia-
365 tion is sieved out, with volcanism being more frequent and voluminous in the eastern
366 systems (Krýsuvík and Brennisteinsfjöll) within the peninsula. As discussed in Sinton

367 [et al \(2005\)](#), what controls high-volume eruptions is either tapping of large magma
368 reservoirs or tapping reservoirs with continuous recharge. The former would favor
369 eruptions with homogeneous compositions and potentially overpressurized eruptions
370 resulting in high initial effusion rates, while the later more heterogeneous compositions
371 tapping different mantle sources and with more stable effusion rates, as in Fagradals-
372 fjall eruption in 2021 ([Halldórsson et al, 2022](#); [Pedersen et al, 2022](#)). [Jakobsson et al](#)
373 ([1978](#)) points out that the olivine tholeiite shields and the tholeiite fissure eruptions
374 on Reykjanes do indeed have more homogeneous compositions indicating origin within
375 magma storage systems while the picrites have more heterogeneous compositions, indi-
376 cating tapping of deeper mantle sources. Jakobsson posited that the surface expression
377 of shallow magma reservoirs was the pronounced graben structures in the volcanic
378 systems, the occurrences of geothermal fields and the evolved composition of the lava
379 fields. He also postulates the role of crustal thickness permitting storage, that is, most
380 tholeiitic lava flows have originated near the central areas of the Peninsula around the
381 spreading center, where crustal thicknesses are greater. The eruption forming Sand-
382 fellshæð shield within the western province, could be evidence of this (Fig. 4). It can
383 be added that crustal thickness also increases rapidly inland ([Darbyshire et al, 2000](#))
384 and the eastern part of Reykjanes is likely controlled by greater storage capability
385 within the crust, increasing the potential for long-lived eruptions. Yet this same fac-
386 tor would mean eruption frequency is lower in the easternmost system, the Hengill
387 system, where more time is needed to replenish larger reservoirs.

388 5.2 Time of formation of the lava shields

389 The MOR values attained for the shield eruptions, e.g. $31 \text{ m}^3/\text{s}$ for Selvogsheiði to 102
390 m^3/s for Heðin Há is considerably higher than usually attributed to shield eruptions,
391 which are often given to be in the range of $5\text{--}15 \text{ m}^3/\text{s}$ (e.g. [Rossi and Gudmunds-](#)
392 [son, 1996](#)). A lower value of T_{surf} , 50°C , is used for the lava shields, a temperature

393 that would be reached in 3.6 years according to equation 2, as it is assumed that lava
394 shield-forming eruptions are long-lived. This can be inferred from their greater vol-
395 ume and geometry with a steeper cone and an circumscribing apron (Thordarson and
396 Sigmarsson, 2009), with mature lava fields and crusts - displaying tumuli and lava-rise
397 features (Rossi and Gudmundsson, 1996), and with evidence well-developed internal
398 pathways or tubes (Peterson et al, 1994). The MOR nevertheless will be underesti-
399 mated if the eruption duration were shorter, however, not greatly as T_{surf} of 75°C
400 reached in 1.3 years, is only slightly higher, and within the uncertainties of this type
401 of assessment. However, The usage of lower T_{surf} as of 30°C , that would be appli-
402 cable for eruptions lasting over 17 years, is a time frame that is deemed unrealistic
403 because the lava shields are low profile half-shields, in which most have low volumes
404 ($<3 \text{ km}^3$) compared to other Icelandic counterparts. The dimensions and thicknesses
405 of the lobes (100 's m wide and 1–10 m thick) in some of the shields also suggest larger
406 eruptions, e.g. Hrótagjá (Óskarsson, 2005), which are comparable to the distal flows
407 within Holuhraun lava field that had MOR $90 \text{ m}^3/\text{s}$ (Pedersen et al, 2017). Furthur-
408 more, the length of the flows, such as, Leitahraun that reaches over 20 km seems to
409 imply relatively high effusion rates, and from the width and thickness of the largest
410 lava tubes, e.g., in Raufarhólshellir in Leitahraun, with diameter up to 10 m in height
411 and 30 m in width, that seems to have easily accommodated the estimated MOR of
412 $200 \text{ m}^3/\text{s}$.

413 Although the estimated MOR accounts to some extent for the total volume erupted,
414 the vertical buildup of the shield may be oblivious to the heat model, which does not
415 account for overbank surface flows at the crater, or resurfacing with the formation of
416 new flows as the lava reaches its cooling-limit. With time, effusion rates may decline
417 and flows may pile around the vent as observed in the half-shields of Surtsey island
418 (Thordarson et al, 2009). But as seen from these MOR and the volume estimates (see
419 Table S1), shields in the lower MOR range as Selvogsheiði could have formed within

420 2 years accounting for a decline in effusion rates, and larger shields such as Heðin
421 Há would be in less than 5 years due to higher MOR. Others, such as Leitahraun
422 could have formed within a year if the flow was unidirectional at each given time as
423 discussed above and with a MOR in the range of 200 m³/s. Hrútagjá lava flows could
424 have widen to its size in 2–3 years. This assessment would shed new light on shield
425 forming volcanism in Iceland but better constraints on the architecture and buildup
426 of these shields will help improve the eruption duration.

427 It could also be argued from the general low MOR of most eruptions on Reykjanes
428 that the storage capacity of the Reykjanes peninsula is low, and that would also favour
429 rather short cycles of shield construction. In contrast, the northern segment of the
430 western volcanic zone that is located on a thicker crust, has formed larger shields that
431 erupt at lower frequency (Eason and Sinton, 2009).

432 5.3 Implications for hazard assessment

433 The isopach map of Figure 4 shows that the locus of volcanism with higher MOR,
434 where volcanism tends to be established and form mature vents and craters, clusters
435 near the central areas of the peninsula, and align with the spreading ridge where,
436 potentially, magma influx is greater, and that the peripheries of the fissure swarms
437 have lower MOR. This implies that eruptions within the higher range of MOR are
438 likely to be confined to the central areas of the peninsula, away from most urban
439 centers, giving time for evacuation and planning.

440 The MOR is only an indication of the average effusion rate, whilst many eruptions
441 begin with effusion rates that are much higher, e.g., if the initial rate is responding
442 to an overpressurized reservoir. The eruption of Fagradalshraun in 2021 was different,
443 and gave new insight into eruptions with sustained low effusion rates, whereby the
444 initial effusion rate was the same as the MOR (Pedersen et al, 2022). Thus, it is not
445 unlikely that other eruptions at Reykjanes behaved similarly. But the Sundhnúkgígur

446 eruptions erupted overpressurized that quickly declined and ceased in only 1–2 days,
 447 yet their areal coverage was 70% of the area covered by Fagradalshraun in six months.
 448 If some of the largest events erupted lava from pressurized reservoirs, such as the
 449 largest early Holocene eruptions of Reykjanes e.g., Heiðin Há and Leitahraun, could
 450 have had initial effusion rates much higher or in the range of 300–500 m³/s as in
 451 Holuhraun 2014–15, rates that would eventually decline with time. These rates would
 452 result in fast-advancing lava flows and impose considerable danger to the population
 453 of the peninsula.

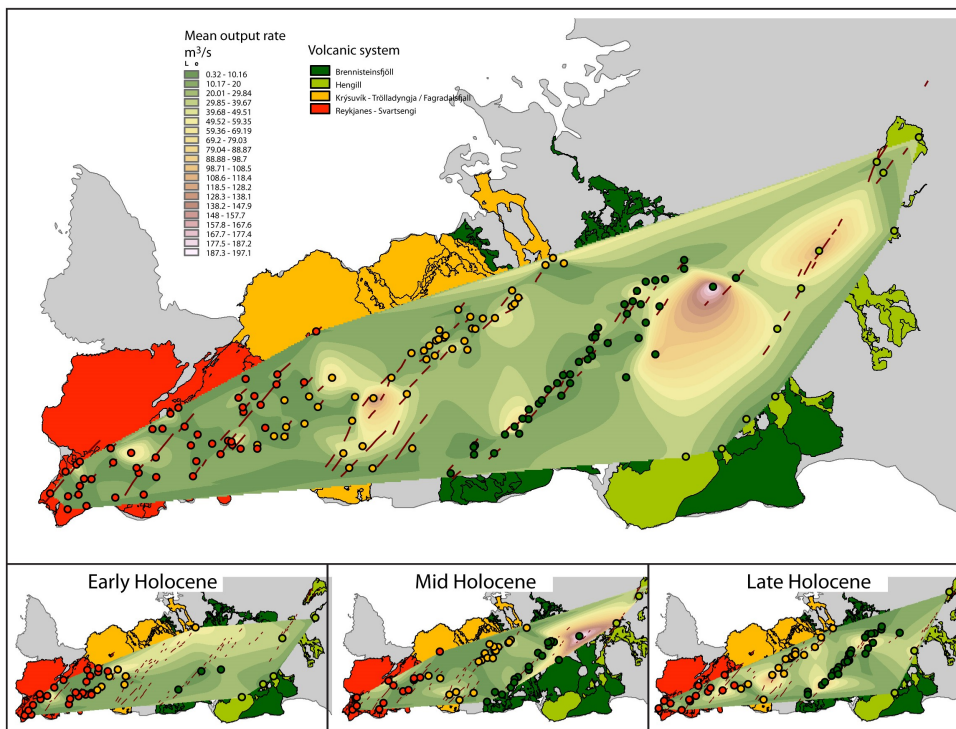


Fig. 4 Isopach maps with the MOR distribution showing the eruption potential within the Reykjanes peninsula. Interpolation Natural neighbor.

454 6 Conclusion

455 The approach presented for calculating the mean output rates of past effusive erup-
456 tions provides first-order assessment of the scale and magnitude of effusive eruptions,
457 even extending the application to a regional scale evaluating the eruption capacity of
458 a volcanic area. The method is derived from a theoretical approximation of effusive
459 eruptions with a range of compositions and emplacement styles and not on a case-to-
460 case basis, thereafter the heat model shows to be applicable to other volcanic regions.
461 The MOR of the 154 postglacial monogenetic eruptions on the Reykjanes peninsula
462 gives moderate background activity under $50 \text{ m}^3/\text{s}$, but with recurring volcanism in
463 the range of $50\text{--}200 \text{ m}^3/\text{s}$. The majority of these yield relatively short to medium-
464 lived eruptions (< 1 year), while a few extended to be long-lived (a few years) and
465 formed shields, the activity mostly confined to the early and middle Holocene. In
466 recent decades, volcanism has comprised moderately large fissure eruptions of short
467 duration rather than eruptions of long duration. Besides the role of isostatic adap-
468 tations affecting magma production following deglaciation, magma is seen to accent
469 directly from lower crustal areas and form primitive heterogeneous lava fields or stall
470 in storage systems which the role of crustal catchments in central and eastern regions
471 of the peninsula where the crust is thickest.

472 References

- 473 Andrew RE, Gudmundsson A (2007) Distribution, structure, and formation of
474 Holocene lava shields in Iceland. *J Volcanol Geotherm Res* 168(1–4):137–154
- 475 Bilotta G, Cappello A, Hérault A, et al (2012) Sensitivity analysis of the magflow
476 cellular automaton model for lava flow simulation. *Environmental Modelling and*
477 *Software* 35:122–131. <https://doi.org/10.1016/j.envsoft.2012.02.015>

- 478 Calvari S, Neri M, Pinkerton H (2002) Effusion rate estimations during the 1999
479 summit eruption on Mount Etna, and growth of two distinct lava flow fields. J
480 Volcanol Geotherm Res 119(1-4):107–123
- 481 Cappello A, Hérault A, Bilotta G, et al (2016) Magflow: a physics-based model for
482 the dynamics of lava-flow emplacement. <https://doi.org/10.1144/SP426.16>, URL
483 <https://doi.org/10.1144/SP426.16>
- 484 Chevrel MO, Labroquère J, Harris AJL, et al (2018) Pyflowgo: An open-source plat-
485 form for simulation of channelized lava thermo-rheological properties. Computers
486 and Geosciences 111:167–180. <https://doi.org/10.1016/j.cageo.2017.11.009>
- 487 Darbyshire FA, Whilte RS, Priestley KF (2000) Structure of the crust and uppermost
488 mantle of Iceland from a combined seismic and gravity study. Earth Planet Sci Lett
489 181:409–428
- 490 Eason DE, Sinton JM (2009) Lava shields and fissure eruptions of the Western Volcanic
491 Zone, Iceland, evidence for magma chambers and crustal interaction. J Volcanol
492 Geotherm Res 186:331–348
- 493 Edwards B, Magnusson E, Thordarson T, et al (2012) Interactions between lava and
494 snow/ice during the 2010 Fimmvörðuháls eruption, south-central Iceland. J Geophys
495 Res 117(B4):B04302–
- 496 Einarsson M (1984) Climate of Iceland. In: van Loon H (ed) World Survey of
497 Climatology:15: Climates of the Oceans. Elsevier, Amsterdam, p pp. 673–697
- 498 Einarsson P (1991) Umbrotin við Kröflu 1975–89 (in icelandic). In: Gardarsson A,
499 Einarsson A (eds) Náttúra Mývatns. Hið Íslenska Náttúrufræðifélag, p 97–139

- 500 Einarsson S, Jóhannesson H, Sveinbjörnsdóttir AE (1991) Kapelluhraun og gátan um
501 aldur Hellnahrauns (the krísuvík fires ii . Age of the Kapelluhraun and Hellnahraun
502 lava flows, Reykjanes peninsula, Southwest Iceland). *Jökull* 41:61–80
- 503 Gee MAM (1998) Volcanology and Geochemistry of Reykjanes peninsula: Plume-Mid
504 Ocean Ridge interaction. PhD-Thesis: Royal Holloway University of London p 315
505 pp.
- 506 Geshi N (2005) Structural development of dike swarms controlled by the change
507 of magma supply rate: the cone sheets and parallel dike swarms of the Miocene
508 Otoge igneous complex, Central Japan. *Journal of Volcanology and Geothermal*
509 *Research* 141(3):267–281. <https://doi.org/10.1016/j.jvolgeores.2004.11.002>, URL
510 <https://www.sciencedirect.com/science/article/pii/S0377027304003518>
- 511 Geshi N, Browning J, Kusumoto S (2020) Magmatic overpressures, volatile exsolution
512 and potential explosivity of fissure eruptions inferred via dike aspect ratios. *Scientific*
513 *Reports* 10(1):9406. <https://doi.org/10.1038/s41598-020-66226-z>, URL [https://doi.](https://doi.org/10.1038/s41598-020-66226-z)
514 [org/10.1038/s41598-020-66226-z](https://doi.org/10.1038/s41598-020-66226-z)
- 515 Gudmundsson A (1986) Mechanical aspects of postglacial volcanism and tectonics
516 of the Reykjanes Peninsula, southwest Iceland. *J Geophys Res* 91(B12):12711–
517 12721. <https://doi.org/10.1029/JB091iB12p12711>, URL [https://doi.org/10.1029/](https://doi.org/10.1029/JB091iB12p12711)
518 [JB091iB12p12711](https://doi.org/10.1029/JB091iB12p12711)
- 519 Gudmundsson A (2006) How local stresses control magma-chamber ruptures, dyke
520 injections, and eruptions in composite volcanoes. *Earth-Science Reviews* 79(1):1–31.
521 <https://doi.org/10.1016/j.earscirev.2006.06.006>, URL [https://www.sciencedirect.](https://www.sciencedirect.com/science/article/pii/S001282520600078X)
522 [com/science/article/pii/S001282520600078X](https://www.sciencedirect.com/science/article/pii/S001282520600078X)

- 523 Halldórsson SA, Marshall EW, Caracciolo A, et al (2022) Rapid shifting of a
524 deep magmatic source at fagradalsfjall volcano, iceland. *Nature* 609(7927):529–
525 534. <https://doi.org/10.1038/s41586-022-04981-x>, URL <https://doi.org/10.1038/s41586-022-04981-x>
526
- 527 Harris A, Rowland S (2001) FLOWGO: a kinematic thermo-rheological model for lava
528 flowing in a channel. *Bull Volc* 63(1):20–44
- 529 Harris A, Murray J, Aries S, et al (2000) Effusion rate trends at Etna and Krafla
530 and their implications for eruptive mechanisms. *J Volcanol Geotherm Res* 102(3–
531 4):237–269
- 532 Harris A, Dehn J, Calvari S (2007) Lava effusion rate definition and measurement: a
533 review. *Bull Volc* 70(1):1–22
- 534 Harris A, Steffke A, Calvari S, et al (2011) Thirty years of satellite-derived lava dis-
535 charge rates at etna: Implications for steady volumetric output. *J Geophys Res*
536 116(B8)
- 537 Harris AJL, Rowland SK (2009) Effusion rate controls on lava flow length and the role
538 of heat loss: a review. *Studies in volcanology: The legacy of George Walker Special*
539 *Publications of IAVCEI* (2):33–51
- 540 Hartley M, Maclennan J (2018) Magmatic Densities Control Erupted Volumes in
541 Icelandic Volcanic Systems. *Frontiers in Earth Science* 6
- 542 Hon K, Kauahikaua J, Delinger R, et al (1994) Emplacement and inflation of pahoehoe
543 sheet flows: Observations and measurements of active lava flows on Kilauea Volcano,
544 Hawaii. *Geol Soc Am Bull* 106(3):351–370
- 545 Jakobsson S (2013) Vesturgosbeltið (western volcanic zone). *Náttúruvá á Íslandi* pp
546 359–365

- 547 Jakobsson SP, Jónsson J, Shido F (1978) Petrology of the Western Reykjanes Penin-
548 sula, Iceland. *J Petrology* 19(4):669–705. [https://doi.org/10.1093/](https://doi.org/10.1093/petrology/19.4.669)
549 [petrology/19.4.669](https://doi.org/10.1093/petrology/19.4.669), URL [https://doi.org/10.1093/](https://doi.org/10.1093/petrology/19.4.669)
- 550 Jull M, McKenzie D (1996) The effect of deglaciation on mantle melting beneath
551 Iceland. *J Geophys Res* 101:21,815–21,828
- 552 Jóhannesson H, Einarsson S (1988a) Aldur Illahrauns við Svartsengi (Age of the
553 Illahraun lava at Svartsengi). *Fjölrit Náttúrufræðistofnunar* 7:12
- 554 Jóhannesson H, Einarsson S (1988b) Krýsuvíkureldar. i: Aldur Ögmundarhrauns og
555 miðaldalagsins (The Krýsuvík fires i: Age of the Ögmundarhraun lava and the
556 medieval tephra layer). *Jökull* pp 71–87
- 557 Jónsson J (1978) Geological map of Reykjanes Peninsula (Jarðfræðikort af Reyk-
558 janesskaga). Orkustofnun Jarðhitadeild 7831
- 559 Keiding M, Lund B, Árnadóttir T (2009) Earthquakes, stress, and strain along an
560 obliquely divergent plate boundary: Reykjanes peninsula, southwest iceland. *J Geo-*
561 *phys Res* 114(B9). <https://doi.org/10.1029/2008JB006253>, URL [https://doi.org/](https://doi.org/10.1029/2008JB006253)
562 [10.1029/2008JB006253](https://doi.org/10.1029/2008JB006253)
- 563 Lopes R, Guest JE (1982) Lava flows on etna, a morphometric study. In: Coradini A,
564 Fulchignoni M (eds) *The Comparative Study of the Planets*. Springer Netherlands,
565 Dordrecht, pp 441–458
- 566 Maclennan J, Jull M, McKenzie D, et al (2002) The link between volcanism and
567 deglaciation in Iceland. *Geochem-Geophys-Geosyst* 3(11):1–25
- 568 Mériaux C, Jaupart C (1998) Dike propagation through an elastic plate.
569 <https://doi.org/10.1029/98jb00905>, URL <https://www.scopus.com/inward/record>.

570 [uri?eid=2-s2.0-0000195406&doi=10.1029%2f98jb00905&partnerID=40&md5=](https://doi.org/10.1029/2f98jb00905&partnerID=40&md5=1f15147ce340d0c8b04d145f3e5b94d8)
571 [1f15147ce340d0c8b04d145f3e5b94d8](https://doi.org/10.1029/2f98jb00905&partnerID=40&md5=1f15147ce340d0c8b04d145f3e5b94d8)

572 Newton I (1929) The mathematical beginnings of natural philosophy optics. Optical
573 Lectures, (Selected Topics) Leningrad pp 66–71

574 Óskarsson B (2005) Lava-rise structures in pahoehoe and a'a: Examples from the
575 Hrótagjá lava shield and Kapelluhraun aa flow field on the Reykjanes peninsula.
576 BS thesis p 115 pp

577 Pedersen GBM, Höskuldsson A, Dürig T, et al (2017) Lava field evolution and emplace-
578 ment dynamics of the 2014-2015 basaltic fissure eruption at Holuhraun, Iceland.
579 Journal of Volcanology and Geothermal Research 340:155–169

580 Pedersen GBM, Belart JMC, Magnússon E, et al (2020) Hekla Volcano, Iceland, in
581 the 20th Century: Lava Volumes, Production Rates, and Effusion Rates. Geophys
582 Res Lett 45(4):1805–1813

583 Pedersen GBM, Belart JMC, Óskarsson BV, et al (2022) Volume, Effu-
584 sion Rate, and Lava Transport During the 2021 Fagradalsfjall Eruption:
585 Results From Near Real-Time Photogrammetric Monitoring. Geophys Res Lett
586 49(13):e2021GL097125. <https://doi.org/10.1029/2021GL097125>, URL <https://doi.org/10.1029/2021GL097125>

588 Pedersen GBM, Pfeffer MA, Barsotti S, et al (2023) Lava flow hazard modeling dur-
589 ing the 2021 fagradalsfjall eruption, iceland: applications of mrlavaloba. NHESS
590 23(9):3147–3168. <https://doi.org/10.5194/nhess-23-3147-2023>, URL <https://nhess.copernicus.org/articles/23/3147/2023/>

592 Pedersen GBM, Belart JMC, Óskarsson BV, et al (2024) Volume, effusion rates and
593 lava hazards of the 2021, 2022 and 2023 reykjanes fires: Lessons learned from

594 near real-time photogrammetric monitoring. EGU General Assembly 2024, Vienna,
595 Austria 14–19 Apr 2024 pp EGU24–10724

596 Peterson D, Holcomb R, Tilling R, et al (1994) Development of lava tubes in the light
597 of observations at Mauna Ulu, Kilauea Volcano, Hawaii. *Bull Volc* 56(5):343–360–

598 Pieri DC, Baloga SM (1986) Eruption rate, area, and length relationships for some
599 Hawaiian lava flows. *J Volcanol Geotherm Res* 30(1–2):29–45

600 Pinkerton H, Sparks R (1976) The 1975 sub-terminal lavas, Mount Etna: a case history
601 of the formation of a compound lava field. *J Volcanol Geotherm Res* 1(2):167–182

602 Rees Jones DW, Rudge JF (2020) Fast magma ascent, revised estimates from the
603 deglaciation of Iceland. *Earth and Planetary Science Letters* 542:116324. <https://doi.org/10.1016/j.epsl.2020.116324>, URL <https://www.sciencedirect.com/science/article/pii/S0012821X20302685>
604 [https://www.sciencedirect.com/science/](https://www.sciencedirect.com/science/article/pii/S0012821X20302685)
605 [article/pii/S0012821X20302685](https://www.sciencedirect.com/science/article/pii/S0012821X20302685)

606 Rossi MJ, Gudmundsson A (1996) The morphology and formation of flow-lobe tumuli
607 on Icelandic shield volcanoes. *J Volcanol Geotherm Res* 72(3–4):291–308

608 Sigmundsson F (2006) *Iceland Geodynamics - Crustal Deformation and Divergent*
609 *Plate Tectonics*. Praxis Publishing

610 Sinton J, Grönvold K, Sæmundsson K (2005) Postglacial eruptive history of the
611 Western Volcanic Zone, Iceland. *Geochem Geophys Geosyst* 6(12):Q12009–

612 Soule S, Cashman K, Kauahikaua J (2004) Examining flow emplacement through the
613 surface morphology of three rapidly emplaced, solidified lava flows, Kilauea Volcano,
614 Hawai'i. *Bull Volc* 66(1):1–14

615 Sparks RSJ, Pinkerton H (1978) Effect of degassing on rheology of basaltic lava. *Nature*
616 276(5686):385–386

- 617 Sæmundsson K, Sigurgeirsson M (2013) Reykjaneskagi (Reykjanes peninsula). Náttúruvísindisfréttir 44(4):379–401
- 618 túruvísindisfréttir 44(4):379–401
- 619 Sæmundsson K, Sigurgeirsson M, Hjartarson A, et al (2016) Geological map of
620 Southwest Iceland. 1:000 000 (2nd edition). Reykjavík: Iceland GeoSurvey
- 621 Sæmundsson K, Sigurgeirsson M, Friðleifsson G (2020) Geology and structure of
622 the Reykjanes volcanic system, Iceland. Journal of Volcanology and Geothermal
623 Research 391:106501
- 624 Thordarson T, Self S (1993) The Laki (Skaftár Fires) and Grímsvötn eruptions in
625 1783–1785 I. Bull Volc 55(4):233–263
- 626 Thordarson T, Sigmarsson O (2009) Effusive activity in the 1963–1967 Surtsey eruption,
627 Iceland: flow emplacement and growth of small lava shields. In: Thordarson T,
628 Larsen G, Rowland SK, et al (eds) Studies in Volcanology: The Legacy of George
629 Walker. 2, IAVCEI, p 53–84
- 630 Thordarson T, Rampino M, Keszthelyi LP, et al (2009) Effects of megascale eruptions
631 on Earth and Mars. Geological Society of America Special Papers 453:37–53
- 632 Tibaldi A (2015) Structure of volcano plumbing systems: A review of multi-
633 parametric effects. Journal of Volcanology and Geothermal Research 298:85–135.
634 <https://doi.org/10.1016/j.jvolgeores.2015.03.023>, URL <https://www.sciencedirect.com/science/article/pii/S0377027315000992>
- 635 <https://www.sciencedirect.com/science/article/pii/S0377027315000992>
- 636 Vicari A, Cirauco A, Del Negro C, et al (2009) Lava flow simulations using discharge
637 rates from thermal infrared satellite imagery during the 2006 etna eruption. Natural
638 Hazards 50(3):539–550. <https://doi.org/10.1007/s11069-008-9306-7>, URL <https://doi.org/10.1007/s11069-008-9306-7>
- 639 <https://doi.org/10.1007/s11069-008-9306-7>

- 640 Voigt JRC, Hamilton CW, Scheidt SP, et al (2021) Geomorphological char-
641 acterization of the 2014-2015 holuhraun lava flow-field in iceland. Journal
642 of Volcanology and Geothermal Research 419:107278. [https://doi.org/10.1016/](https://doi.org/10.1016/j.jvolgeores.2021.107278)
643 [j.jvolgeores.2021.107278](https://doi.org/10.1016/j.jvolgeores.2021.107278), URL [https://www.sciencedirect.com/science/article/pii/](https://www.sciencedirect.com/science/article/pii/S0377027321001074)
644 [S0377027321001074](https://www.sciencedirect.com/science/article/pii/S0377027321001074)
- 645 Walker GPL (1973) Length of lava flows. Philosophical Transactions of the Royal
646 Society 274:107–118